Can Steric Effects Induce the Mechanism Switch in the Rhodium-Catalyzed Imine Boration Reaction? A Density Functional and ONIOM Study

Valentin P. Ananikov,[†,‡] Robert Szilagyi,[‡,§] Keiji Morokuma,*[,‡] and Djamaladdin G. Musaev*[,‡]

N. D. Zelinsky Institute of Organic Chemistry, Russian Academy of Sciences, Leninsky Prospect 47, Moscow 119991, Russia, and Cherry L. Emerson Center for Scientific Computation and Department of Chemistry, Emory University, Atlanta, Georgia 30322

Received October 29, 2004

Combined density functional and ONIOM studies have been performed to investigate the mechanism of rhodium-catalyzed boration of imines. Catalytic imine boration has been found to proceed via the following stages: (1) oxidative addition of B−B to the Rh complex, (2) imine coordination, (3) migratory insertion of the imine into the rhodium−boron (Rh−B) bond, and (4) β-hydrogen elimination to give a monoboration product or carbon−boron (C−B) bond formation to yield a diboration product. The choice of the final stage depends on the structure of the imine and boration reagent. Bulky substrate molecules facilitate C−H bond activation and retard C−B bond formation, while in the absence of sterical hindrance C−B bond formation is preferred over C−H bond activation. The present study is the first that outlines the mechanistic differences in C=C and C=N bond boration and rationalizes the effect of bulky substituents on the mechanism of imine boration reaction. The expected difference in regioselectivity between imine and alkene boration is also discussed.

1. Introduction

Transition metal catalyzed hydroboration and diboration reactions are of great importance in modern chemistry as efficient tools for chemo-, stereo-, regio-, and enantioselective preparation of organoboronic compounds,[1,2] which are useful reagents in various cross-coupling reactions and have already found widespread application in synthesis.[3] Understanding the mechanism and factors controlling these fascinating reactions has a great importance in designing new and more efficient processes. Comprehensive experimental and theoretical studies are required to solve issues related to these processes.

Starting with the first discovery of the transition metal catalyzed alkene hydroboration,[4] Rh(I) complexes are frequently employed in various borylation reactions.[1,2] A very interesting feature of the Rh-catalyzed reactions concerns competitive hydroboration versus dehydrogenative borylation reactions.[5,6]

Earlier theoretical studies of the mechanisms of H−B and B−B addition reactions to alkenes and alkynes have shown that these reactions proceed through the sequence of (1) H−B and B−B oxidative addition to a transition metal complex, (2) alkene or alkyne coordination to the oxidative addition products followed by insertion into the M−B or M−H bond, and (3) reductive elimination.[7,8] Both associative and dissociative mechanisms of the Rh(I)-catalyzed hydroboration reaction

* To whom correspondence should be addressed. E-mail: dmusaev@emory.edu. Phone: 404-727-2382. E-mail: morokuma@emory.edu. Phone: 404-727-2180.

† N. D. Zelinsky Institute of Organic Chemistry.

‡ Emory University.

§ Present address: Department of Chemistry and Biochemistry, Montana State Univ., Bozeman, MT 59717.

(1) *Catalytic Heterofunctionalization*; Togni, A., Grützmacher, H., Eds.; Wiley-VCH: Weinheim, 2001.

(2) (a) Alonso, F.; Beletskaya, I. P.; Yus, M. *Chem. Rev.* **2004**, *104*, 3079. (b) Crudden, C. M.; Edwards, D. *Eur. J. Org. Chem.* **2003**, 4695. (c) Ishiyama, T.; Miyaura, N. *J. Organomet. Chem.* **2003**, *680*, 3. (d) Beletskaya, I. P.; Moberg, C. *Chem. Rev.* **1999**, *99*, 3435. (e) Irvine, G. J.; Lesley, M. J. G.; Marder, T. B.; Norman, N. C.; Rice, C. R.; Robins, E. G.; Roper, W. R.; Whittell, G. R.; Wright, L. J. *Chem. Rev.* **1998**, *98*, 2685. (f) Beletskaya, I. P.; Pelter, A. *Tetrahedron* **1997**, *53*, 4957. (g) Burgess, K.; Ohlmeyer, M. J. *Chem. Rev.* **1991**, *91*, 1179.

(3) (a) *Metal-catalyzed Cross-coupling Reactions*; Diederich, F., Stang, P. J., Eds.; Wiley-VCH: Weinheim, 1998. (b) Suzuki, A. *J. Organomet. Chem.* **1999**, *576*, 147. (c) Miyaura, N.; Suzuki, A. *Chem. Rev.* **1995**, *95*, 2457.

(4) Männig, D.; Nöth, H. *Angew. Chem., Int. Ed. Engl.* **1985**, *24*, 878.

(5) (a) Coapes, R. B.; Souza, F. E. S.; Thomas, R. L.; Hall, J. J.; Marder, T. B. *Chem. Commun*. **2003**, 614. (b) Murata, M.; Kawakita, K.; Asana, T.; Watanabe, S.; Masuda, Y. *Bull. Chem. Soc. Jpn.* **2002,** *75*, 825. (c) Brown, J. M.; Lloyd-Jones, G. C. *J. Am. Chem. Soc.* **1994**, *116*, 866. (d) Murata, M; Watanabe, S.; Masuda, Y. *Tetrahedron Lett.* **1999**, *40*, 2585. (e) Westcott, S. A.; Marder, T. B.; Baker, R. T. *Organometallics* **1993**, *12*, 975. (f) Baker, R. T.; Calabrese, J. C.; Westcott, S. A.; Nguyen, P.; Marder, T. B. *J. Am. Chem. Soc.* **1993**, *115*, 4367. (g) Brown, J. M.; Lloyd-Jones, G. C. *J. Chem. Soc., Chem. Commun.* **1992**, 710. (h) Evans, D. A.; Fu, G. C.; Hoveyda, A. H. *J. Am. Chem. Soc.* **1992**, *114*, 6671. (i) Evans, D. A.; Fu, G. C.; Andersen, B. A. *J. Am. Chem. Soc.* **1992**, *114*, 6679. (j) Burgess, K.; van der Donk, W. A.; Westcott, S. A.; Marder T. B.; Baker R. T.; Calabrese, J. C. *J. Am. Chem. Soc.* **1992**, *114*, 9350.

(6) See also: (a) Kadlecek, D. E.; Carroll, P. J.; Sneddon, L. G. *J. Am. Chem. Soc.* **2000**, *122*, 10868. (b) Smith, M. R., III *Prog. Inorg. Chem.* **1999**, *48*, 505. (c) Motry, D. H.; Smith, M. R., III. *J. Am. Chem. Soc.* **1995**, *117*, 6615.

(7) (a) Musaev, D. G.; Mebel, A. M.; Morokuma, K. *J. Am. Chem. Soc.* **1994**, *116*, 10693. (b) Dorigo, A. E.; von Rague-Schleyer, P. *Angew. Chem., Int. Ed. Engl.* **1995**, *34*, 115. (c) Widauer, C.; Grützmacher, H.; Ziegler, T. *Organometallics* **2000**, *19*, 2097. (d) Liu, D.; Lin, Z. *Organometallics* **2002**, *21*, 4750.

(8) (a) Cui, Q.; Musaev, D. G.; Morokuma, K. *Organometallics* **1997**, *16*, 1355. (b) Cui, Q.; Musaev, D. G.; Morokuma, K. *Organometallics* **1998**, *17*, 742. (c) Matsubara, T.; Maseras, F.; Koga, N.; Morokuma, K. *J. Phys. Chem.* **1996**, *100*, 2573.

10.1021/om049156o CCC: $30.25
Publication on Web 03/11/2005

Scheme 1. Catalytic Imine Boration Reaction

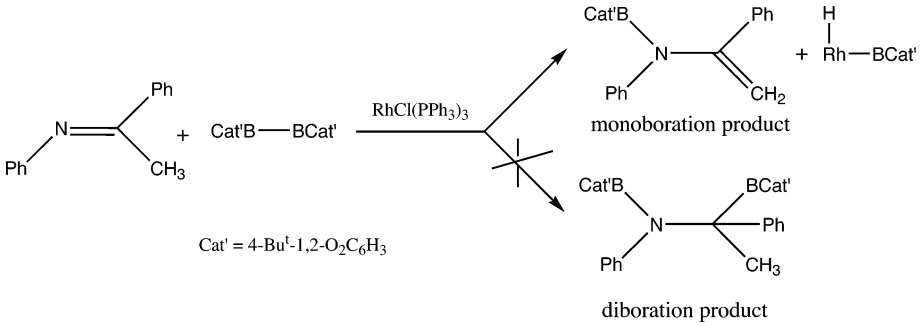

Scheme 2. Real and Model (in circles) Systems Used in the ONIOM Studies

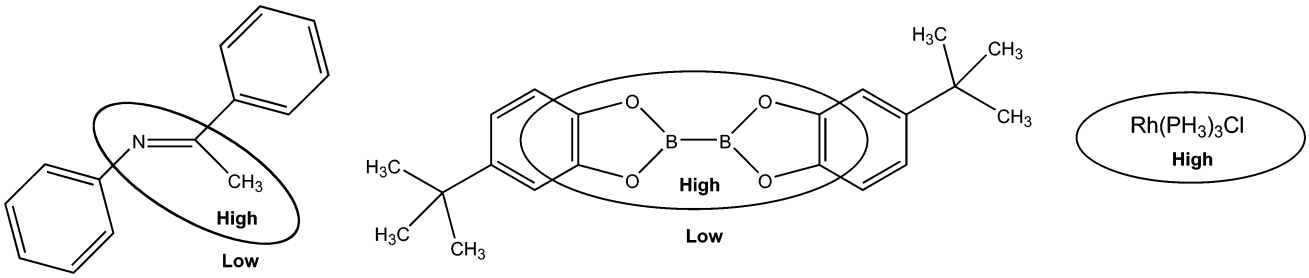

have been analyzed.[7c] Mechanistic studies of the catalytic carbon−boron bond formation involving other borylation approaches have proven the utility of the density functional methods in investigations of these fascinating reactions.[9]

Recently published[10] Rh-catalyzed B−B addition to the C=N bond breaks away from the common framework of catalytic boration reactions and leads to the monoboration compound with a migrated double bond instead of the diboration product (Scheme 1). The reaction proceeded under mild conditions at 25 °C with high selectivity.[10] To understand the mechanism of this reaction and reveal the factors responsible for such unusual reactivity and selectivity, we have performed and report the results of the theoretical density functional and ONIOM studies of the mechanism of these catalytic cycles.

2. Calculation Procedure

In the first stage of our studies we used a simplified model for substrates and catalyst. In these calculations we use $RhCl(PH_3)_3$ as a model catalyst, $(H_2C_2O_2)B-B(H_2C_2O_2)$ as a model Cat′B−BCat′ fragment, and $HN=C(H)CH_3$ as a model imine $PhN=C(Ph)CH_3$. Geometries of the reactants, intermediates, transition states (TSs), and products of this model reaction were optimized using the B3LYP hybrid density functional method[11] and Lanl2DZ basis set[12] supplied with polarization d-functions for C, N, O, B, P, and Cl.[13] Their energetics were improved by using the slightly larger basis set BSI, including the SDD basis set[14] for Rh and the 6-311G(d) basis set[15] for the other atoms.

To incorporate the electronic and steric effects from the substrates missing in the use of small models, in the next stage we have investigated the mechanism of this reaction by taking the entire molecules of the substrates, $PhN=C(CH_3)Ph$ and Cat′B−BCat′, into calculations. In these calculations we use the two-layer ONIOM approach.[16] In the ONIOM partitioning we used the model system described above and presented in Scheme 2 as a first-layer that was treated at the highest, B3LYP/BSI, level. The rest of the substrates were included into the second layer and treated at the relatively low, HF/Lanl2MB level. Therefore, the two-layer ONIOM approach used in the present studies is denoted as ONIOM (B3LYP/BSI: HF/Lanl2MB).

One should note that in both cases (ONIOM and B3LYP calculations) the $Rh(PPh_3)_3Cl$ catalyst was modeled as $Rh(PH_3)_3Cl$. This model has been utilized in several theoretical studies and shown to provide reliable conclusions.[7−9]

In both model and ONIOM studies the normal coordinate analysis has been performed for all stationary points to characterize the TSs and equilibrium structures and to calculate Gibbs free energies (298.15 K, 1 atm, rigid rotor harmonic oscillator approximation). All calculations were performed without symmetry constraints utilizing the Gaussian-03 program.[17]

The energetic parameters of the calculated potential energy surface are listed in Table 1. Chemically more interesting ΔG values will be used in the discussion, and corresponding ΔH

(9) (a) Sumimoto, M.; Iwane, N.; Takahama, T.; Sakaki, S. *J. Am. Chem. Soc.* **2004**, *126*, 10457. (b) Lam, W. H.; Lam, K. C.; Lin, Z.; Shimada, S.; Perutz, R. N.; Marder, T. B. *Dalton Trans.* **2004**, 1556. (c) Tamura, H.; Yamazaki, H.; Sato, H.; Sakaki, S. *J. Am. Chem. Soc.* **2003**, *125*, 16114.

(10) Cameron, T. M.; Baker, T. R.; Westcott, S. A. *Chem. Commun.* **1998**, 2395.

(11) (a) Becke, A. D. *Phys. Rev. A* **1988**, *38*, 3098. (b) Lee, C.; Yang, W.; Parr, R. G. *Phys. Rev. B* **1988**, *37*, 785. (c) Becke, A. D. *J. Chem. Phys.* **1993**, *98*, 5648.

(12) (a) Hay, P. J.; Wadt, W. R. *J. Chem. Phys.* **1985**, *82*, 270. (b) Hay, P. J.; Wadt, *J. Chem. Phys.* **1985**, *82*, 284. (c) Hay, P. J.; Wadt, W. R. *J. Chem. Phys.* **1985**, *82*, 299. (d) Dunning, T. H., Jr.; Hay, P. J. In *Modern Theoretical Chemistry*; . Schaefer, H. F, III, Ed.; Plenum: New York, 1976; Vol. 3, pp 1−28.

(13) (a) Ditchfield, R.; Hehre, W. J.; Pople, J. A. *J. Chem. Phys.* **1971**, **54**, 724. (b) Hehre, W. J. ; Ditchfield, R.; Pople, J. A. *J. Chem. Phys.* **1972**, *56*, 2257.

(14) (a) Schwerdtfeger, P.; Dolg M.; Schwarz, W. H.; Bowmaker, G. A.; Boyd, P. D. W. *J. Chem. Phys.* **1989**, *91*, 1762. (b) Andrae, D.; Haubermann, U.; Dolg, M.; Stoll, H.; Preuss, H. *Theor. Chim. Acta* **1990**, *77*, 123. (c) Bergner, A.; Dolg M.; KŸchle, W.; Stoll, H.; Preuss, H. *Mol. Phys.* **1993**, *80*, 1431.

(15) Krishnan R.; Binkley, J. S.; Seeger, R.; Pople, J. A. *J. Chem. Phys.* **1980**, *72*, 650.

(16) (a) Dapprich, S.; Komáromi, I.; Byun, K. S.; Morokuma, K.; Frisch, M. J. *J. Mol. Struct. (THEOCHEM)* **1999**, 462, 1. (b) Vreven, T.; Morokuma, K. *J. Comput. Chem.* 2000, **21**, 1419.

(17) Frisch, M. J.; et al. *Gaussian 03*, Rev. C1; Gaussian, Inc.: Pittsburgh PA, 2003.

Table 1. Potential Energy Surfaces (in kcal/mol) of the Catalytic Reaction Calculated for the Model Substrates at the B3LYP/Lanl2dz Level and for the Entire Real Substrates at the ONIOM (B3LYP/BSI:HF/Lanl2mb) Levels (in brackets)

structure	ΔE	ΔH	ΔG
1	0.0 [0.0]	0.0 [0.0]	0.0 [0.0]
2	42.0	39.7	29.0
3	29.7	27.9	17.3
4	−3.8	−3.2	9.8
5-TS	9.1	8.9	23.3
6	−12.4	−11.5	1.6
7	−2.5	−1.2	9.5
8-TS	9.8	9.4	10.8
9	−2.5	−2.7	11.9
10	11.0	9.4	10.8
11	38.5	36.3	34.9
12	−4.1	−5.3	−2.5
13	−18.0	−17.5	−4.4
14-TS	3.5	3.2	19.1
15	−23.4	−22.4	−7.0
16-TS	−2.8	−2.4	14.4
17	−11.5	−10.4	3.9
18	−22.2 [−11.3]	−21.2 [−10.1]	−6.1 [10.3]
19-TS	−14.3 [16.1]	−13.9 [16.2]	3.6 [38.2]
20	−20.3 [−3.0]	−19.7 [−1.9]	−3.3 [14.4]
21+2	−2.4 [10.8]	−2.2 [10.8]	−0.7 [15.2]
21+1	−44.4 [−31.2]	−42.0 [−28.9]	−29.6 [−13.5]
22	−19.8 [−14.7]	−20.6 [−16.2]	−5.9 [−1.7]
23	5.7	4.3	20.4
24+25	−17.0 [−11.0]	−19.3 [−13.5]	−16.0 [−9.2]
24+26	−26.6 [−20.2]	−27.0 [−20.7]	−13.5 [−6.1]

values will be given in parentheses. Note that the difference between ΔG and ΔH surfaces reflects entropy contributions. The calculated ONIOM energetics will be given in brackets. First, B3LYP calculations on the full catalytic cycle (Figures 1−3) will be analyzed, followed by discussion of ONIOM calculations of the selected stationary points (Figures 3−5).

3. Results and Discussion

A. DFT Studies for Reactions of Model Substrates. Starting from the initial catalyst **1** (Figure 1) the reaction may proceed through two different pathways, dissociative and associative. The dissociative pathway starts by dissociation of one of the phosphine ligands, leading to the three-coordinated *trans*-$(PR_3)_2RhCl$ or *cis*-$(PR_3)_2RhCl$ (structures **2** and **3**, respectively, given in the Supporting Information, Figure S2) complex and followed by coordination of substrates. Meanwhile, the first step of the associative pathway is substrate coordination to **1**. Here, the latter pathway will be considered first.

The first step of the associative pathway could be coordination of either imine or diboration reagent to **1**. The complex between **1** and imine was found to be unstable and dissociated upon geometry optimization. In contrast, diboration reagent coordination to **1** resulted in weakly bound complexes **4** (with the B−B axis parallel to the P2−Rh−Cl axis) and **7** (with the B−B axis parallel to the P1−Rh−P3 axis) with a Gibbs free energy ΔG (and the enthalpy ΔH in parentheses, both relative to **1** and free reagents) of 9.8 (−3.2) kcal/mol for **4** and 9.5 (−1.2) kcal/mol for **7** (Figure 1, Table 1). The resulting complexes are formally pre-reaction complexes, but the positive values of the Gibbs free energy indicate that neither of them is thermodynamically stable. The B−B oxidative addition starting from **4** goes through the transition state **5-TS** and requires a 13.5 (12.1) kcal/mol activation barrier. Octahedral complex **6** is formed as an oxidative addition product with an energy of 1.6 (−11.5) kcal/mol relative to **1**. Meanwhile, the oxidative addition starting from **7** proceeds via **8-TS**, requires a 14.7 (10.6) kcal/mol activation barrier, and leads to the less stable product **9**, which lies 10.3 (8.8) kcal/mol higher than **6**.

To coordinate an imine molecule, the catalyst now has to create a coordination vacancy. Dissociation of any phosphine ligand from **6** leads to five-coordinate compound **12** with distorted trigonal bipyramidal geometry (B1−Rh−B2 = 69.2°; Figure 1) and is slightly exothermic, −4.1 (−6.2) kcal/mol relative to **6**. In complex **9**, dissociation of phosphine ligands located *trans* to B and Cl ligands leads to five-coordinate compounds **10** and **11**, respectively. On the ΔG surface formation of **10** is exothermic by 1.1 kcal/mol and formation of **11** is endothermic by 23.0 kcal/mol. On the ΔH surface both reactions are endothermic by 12.1 and 39.0 kcal/mol, respectively. As compared to **12**, both **10** and **11** are higher in energy by 13.3 (14.7) and 37.4 (41.6) kcal/mol, respectively (Table 1). Therefore, these compounds will not be discussed further. Instead, we will investigate the transformations from **12**.

Here, one should note that complexes **10**, **11**, and **12** could also be reached by a dissociative pathway. Therefore, at this point, a brief comparison between the associative and dissociative pathways should be given (for details concerning the dissociative pathways, see Supporting Information Figure S2). As was mentioned above, the dissociative pathway starts by dissociation of one of the phosphine ligands, leading to the three-coordinated *trans*-$(PR_3)_2RhCl$ or *cis*-$(PR_3)_2RhCl$ (structures **2** and **3**, respectively). The calculations show that the phosphine dissociation step is thermodynamically unfavorable by 29.0 (39.7) kcal/mol for **2** and 17.3 (27.9) kcal/mol for **3**. Both complexes **2** and **3** may undergo coordination of the diboration reagent followed by B−B oxidative addition to give **12** and **10**, respectively (Figure S2), among which complex **12** is more stable. Thus, both associative and dissociative pathways lead to the same complex **12** as stable intermediate. The associative mechanism is less energy demanding, since the calculated phosphine dissociation energy from complex **1** to form **2** on the dissociative pathway is rather high, 29.0 (39.7) kcal/mol. Therefore, in the further representation of the catalytic cycle only the associative pathway will be drawn.[18]

According to the ΔH energy surface six-coordinated complex **6** is the most stable product of the B−B oxidative addition reaction, while according to the ΔG surface five-coordinated compound **12** is the most stable one (Table 1). In the experimental studies of the B−B oxidative addition to Rh(I), five-coordinated compounds were observed and the structure of these compounds was established with X-ray analysis.[19] Our calculations

(18) Another alternative pathway could involve **3** → **29** → **30-TS** → **10**, followed by isomerization of **10** to **12**. However, since complex **12** is formed as a product, it does not change the conclusions made in the present study.

(19) (a) Clegg, W.; Lawlor, F. J.; Marder, T. B.; Nguyen, P.; Norman, N. C.; Orpen, A. G.; Quayle, M. J.; Rice, C. R.; Robins, E. G.; Scott, A. J.; Souza, F. E. S.; Stringer, G.; Whittell, G. R. *J. Chem. Soc., Dalton Trans.* **1998**, 301. (b) Nguyen, P.; Lesley, G.; Taylor, N. J.; Marder, T. B.; Pickett, N. L.; Clegg, W.; Elsegood, M. R. J.; Norman, N. C. *Inorg. Chem.* **1994**, *33*, 4623.

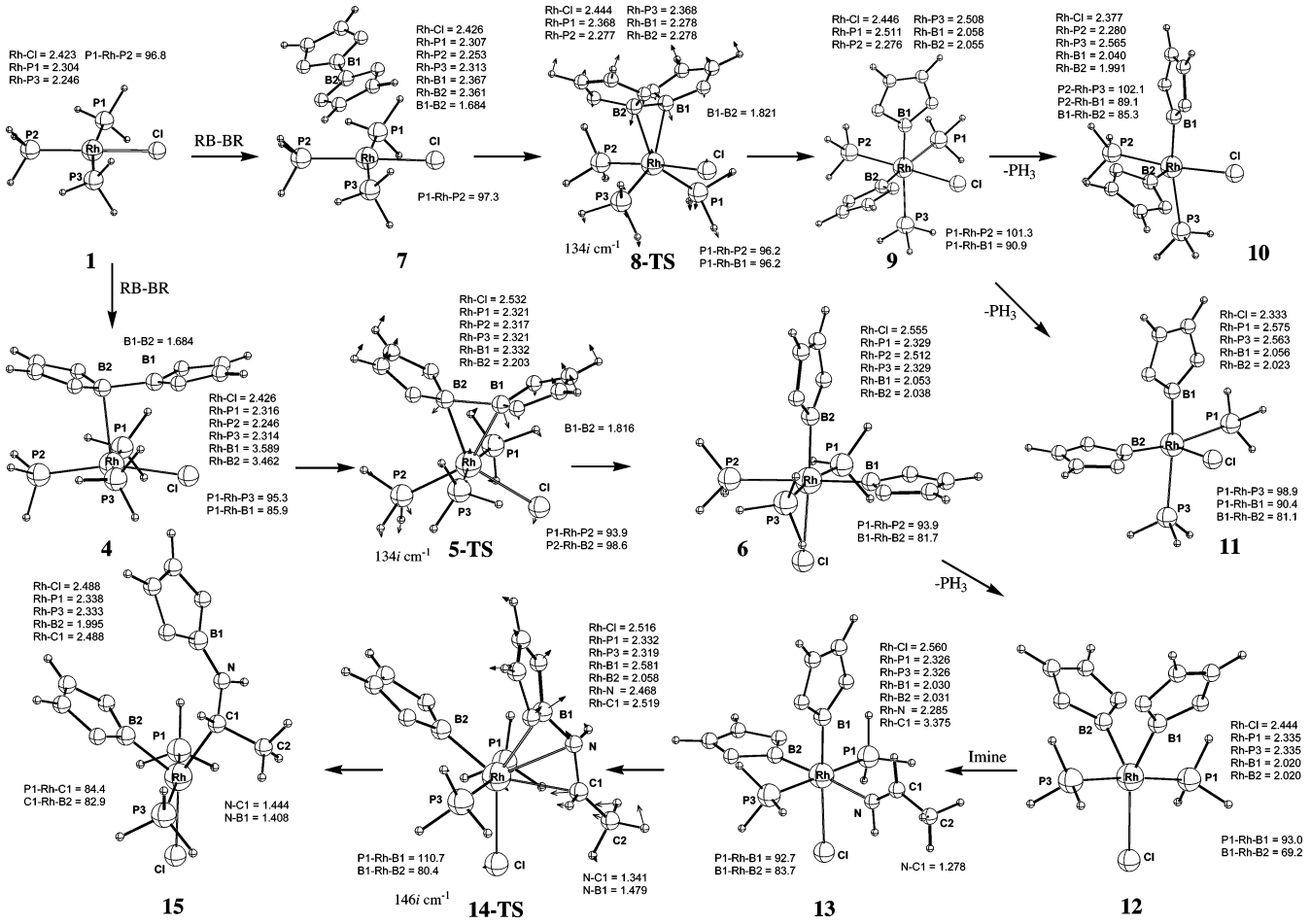

Figure 1. B3LYP-optimized geometry of stationary points **1**−**15** (distances in Å, angles in deg).

are in agreement with the experimental results and emphasize the importance of considering the reaction mechanism on the free energy surface. Calculated geometry parameters for **12**, Rh−Cl = 2.444 Å, Rh−P = 2.335 Å, Rh−B = 2.020 Å (Figure 1), agree very well with experimentally determined values for the [RhCl(PR$_3$)$_2$(Boryl)$_2$] complexes, Rh−Cl = 2.424−2.458 Å, Rh−P = 2.324−2.341 Å, Rh−B = 1.973−2.034 Å,[5e,19] thus confirming the adequate theory level used in the present study.

Noteworthy, the elementary steps involved from reactants to the intermediate **12**, presented above, are the same for both C=N and C=C boration. Therefore, one may expect that the reported difference in the C=N and C=C boration is a result of elementary processes after the intermediate **12**. The next elementary step starting from **12** is coordination of alkene or imine to the transition metal center. To rationalize the reported difference in C=C and C=N boration, let us examine carefully all possible processes staring from **12**. As seen in Scheme 3, where these possible elementary steps are presented, coordination of the alkene C=C bond to the Rh center may lead to two types of η^2-π-complexes, **A** and **C**. Insertion of the C=C double bond in these complexes into the M−B bond via the transition states **TS-A** and **TS**−**C** leads to two products, **B** and **D**, respectively. In many cases the activation barriers for **TS-A** and **TS-C** are of similar magnitude, allowing both products to be obtained (of course, the precise **B/D** ratio depends on R). In contrast to alkenes, imines could coordinate to the Rh center via three different ways: by η^2-π-coordination of the C=N double bond, leading to two complexes, **E** and **F**, and η^1-coordination of the nitrogen loan pair, leading to **G**.

Our calculations show that the η^1-coordination of the nitrogen atom is a preferred form of imine coordination to the rhodium complex. Starting from **12** geometry optimizations of η^2-complexes (like **E** or **F**) converged to **13** (**G**) without energetic barrier (Figure 1). The resulting η^1-complex may undergo two regioselective insertion reactions, leading to compounds **H** and **I** (Scheme 3). However, the activation energies for these reactions are significant: 23.5 (20.7) kcal/mol for the first type of insertion reaction**, 13 → 14-TS → 15** (or **G → TS-G1 → H**), and 60.0 (57.1) kcal/mol for the second one, **13 → 31-TS → 32** (or **G → TS-G2 → I) (**for details see Supporting Information Figure S3). The different nature of **14-TS** and **31-TS** may be clearly rationalized comparing the lengths of broken and formed bonds (such as Rh−N, Rh−C, N−B, and C−B; see Figures 1 and S3). The entire reactions **13 → 14-TS → 15** (or **G → TS-G1 → H**) and **13 → 31-TS → 32** (or **G → TS-G2 → I)** are calculated to be exothermic by 2.6 (4.9) kcal/mol and endothermic by 22.9 (20.4) kcal/mol, respectively.

Thus, from the above-presented discussions one can outline the main differences between alkenes and imines as follows. Two types of orientation of coordinated alkene (**A** and **C**) makes it possible for two insertion reactions (**TS-A** and **TS-C**) leading to different regioselective products (**B** and **D**). The single mode of imine

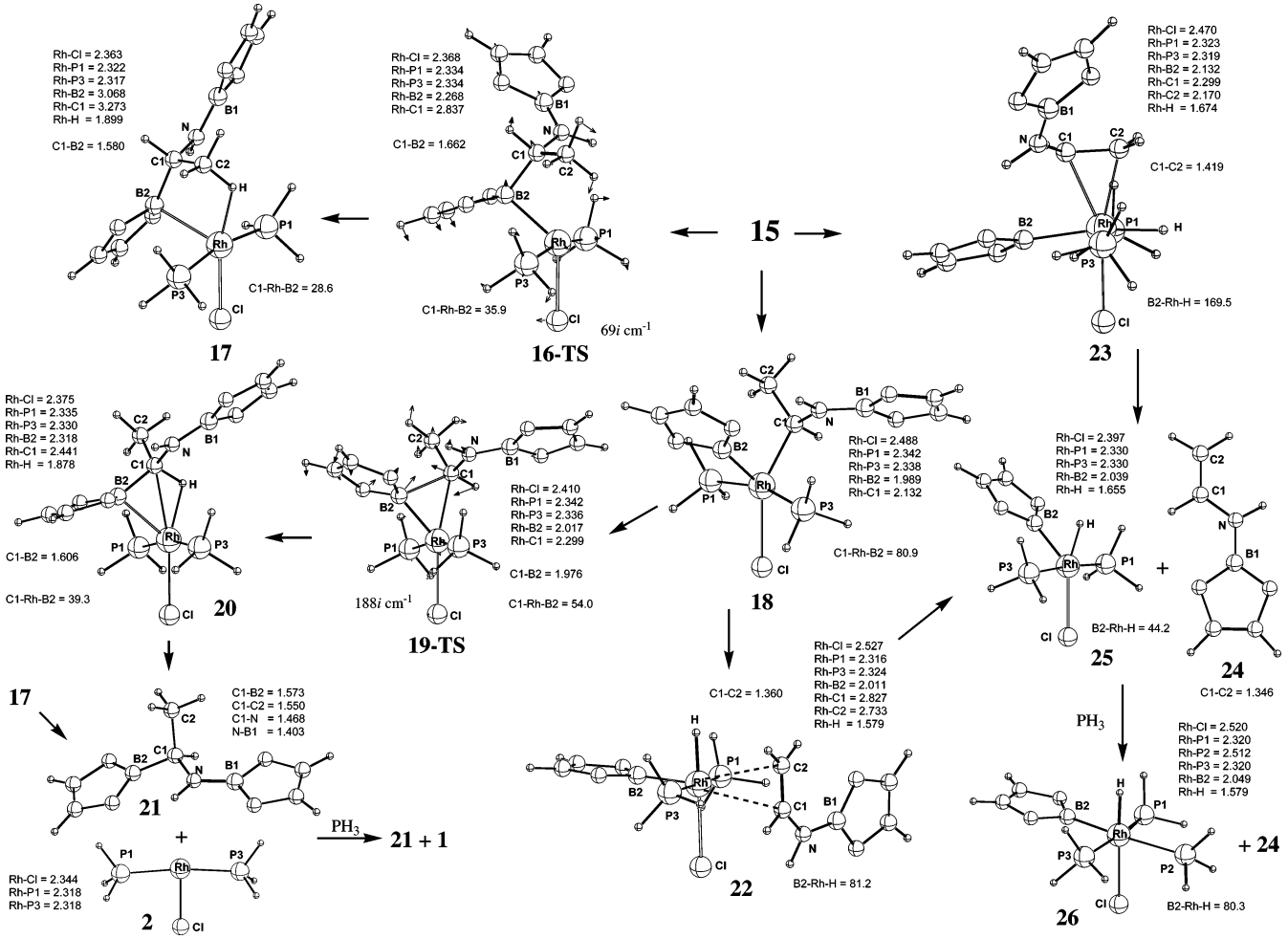

Figure 2. B3LYP-optimized geometry of stationary points **16**−**26** (distances in Å, angles in deg).

ligand coordination strongly prefers the insertion reaction leading to Rh−C and N−B bond formation (**H**). *Therefore, our calculations predict that for the catalytic reaction involving imines higher regioselectivity should be expected. Keeping in mind a general feature of the insertion reaction,*[1−3] *this conclusion may also be valid for the processes involving other metal−element bonds.*

Thus, the first Rh−B insertion step leads to formation of the complex **15** or **18**, with an N−B bond. These complexes are the rotational isomers around the Rh−C1 bond. The energy difference between them is calculated to be only 0.9 (1.2) kcal/mol. As shown previously, the rotation around the σ-bond occurs with a very small energy barrier, and therefore we have not located the transition state for this internal rotation (see Figure 2).

The product, **15** or **18**, of the first Rh−B insertion is an extremely important point on the potential energy surface of the Rh(I)-catalyzed imine C═N bond boration reaction. Indeed, from this point the reaction can selectively proceed to form either diboration or monoboration products.

Within the classical diboration scheme, the process starting from either **15** or **18** is the C−B reductive elimination, which was found to proceed via the transition states **16-TS** and **19-TS**, respectively. The barrier height, 9.7 (7.3) kcal/mol, of the transition state **19-TS** is 11.7 (12.7) kcal/mol lower than that at **16-TS**, which is a result of unfavorable steric repulsion between the boryl ligands in the latter (Figure 2). This difference in the energies between **16-TS** and **19-TS** is consistent with the their geometrical character; **16-TS** is a later TS compared to **19-TS** (cf. Rh−C1, Rh−B2, and C1−B2 bond lengths in Figure 2).

Passage over the barriers at **16-TS** and **19-TS** leads to formation of the intermediates **17** and **20**, respectively (Figure 2). As seen in Table 1, the reaction **15** → **16-TS** → **17** is endothermic by 10.9 (12.0) kcal/mol, while the kinetically more feasible pathway **18** → **19-TS** → **20** is almost thermoneutral, with an energy of reaction of 2.8 (1.5) kcal/mol. The dissociation of these complexes (**17** and **20**) releases the final diboration product **21**. The **17** → **21** + **2** and **20** → **21** + **2** dissociation steps are calculated to be exothermic (4.6 kcal/mol) and endothermic (2.6 kcal/mol), respectively, on the ΔG surface. Both are endothermic by 8.2 and 17.5 kcal/mol, respectively, on the ΔH surface.

Thus, our calculations show that the second boration process of C═N starting from complex **18** proceeds with the 9.7 (7.3) kcal/mol barrier at the transition state **19-TS** and is endothermic only by 2.8 (1.5) kcal/mol. Taking into account the fact that the recoordination of the dissociated phosphine group to **2** to give catalyst **1** will make this second boration process exothermic (the energy of **21** + **1** is −29.6 (−42.0) kcal/mol relative to the start of the catalytic cycle), one may conclude that the formation of the diboration product during this reaction is a feasible process. This conclusion is not in agreement with the available experiment data that

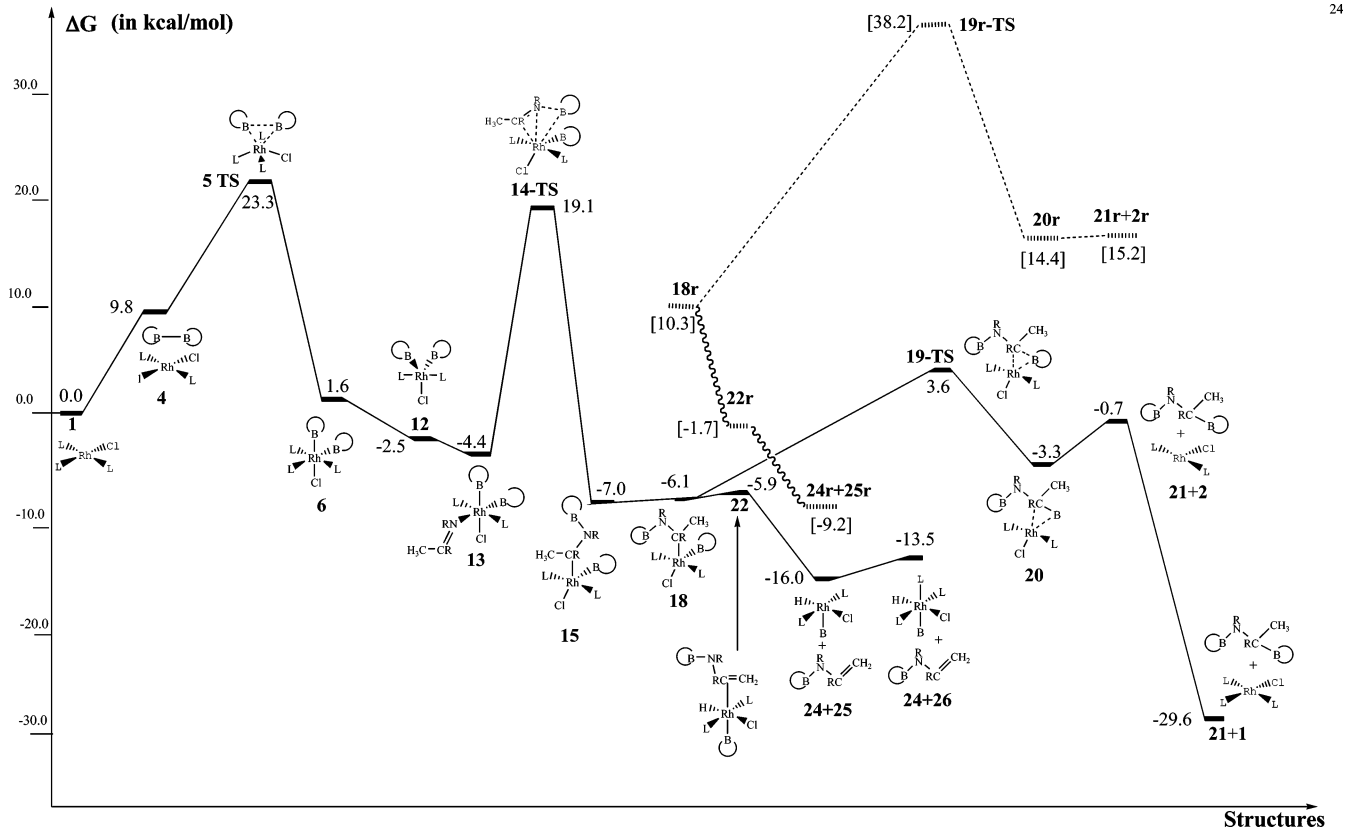

Figure 3. Δ*G* potential energy surfaces of the catalytic cycle for model and real (**r**, dashed and solid lines) reactions, calculated at the B3LYP and ONIOM levels, respectively.

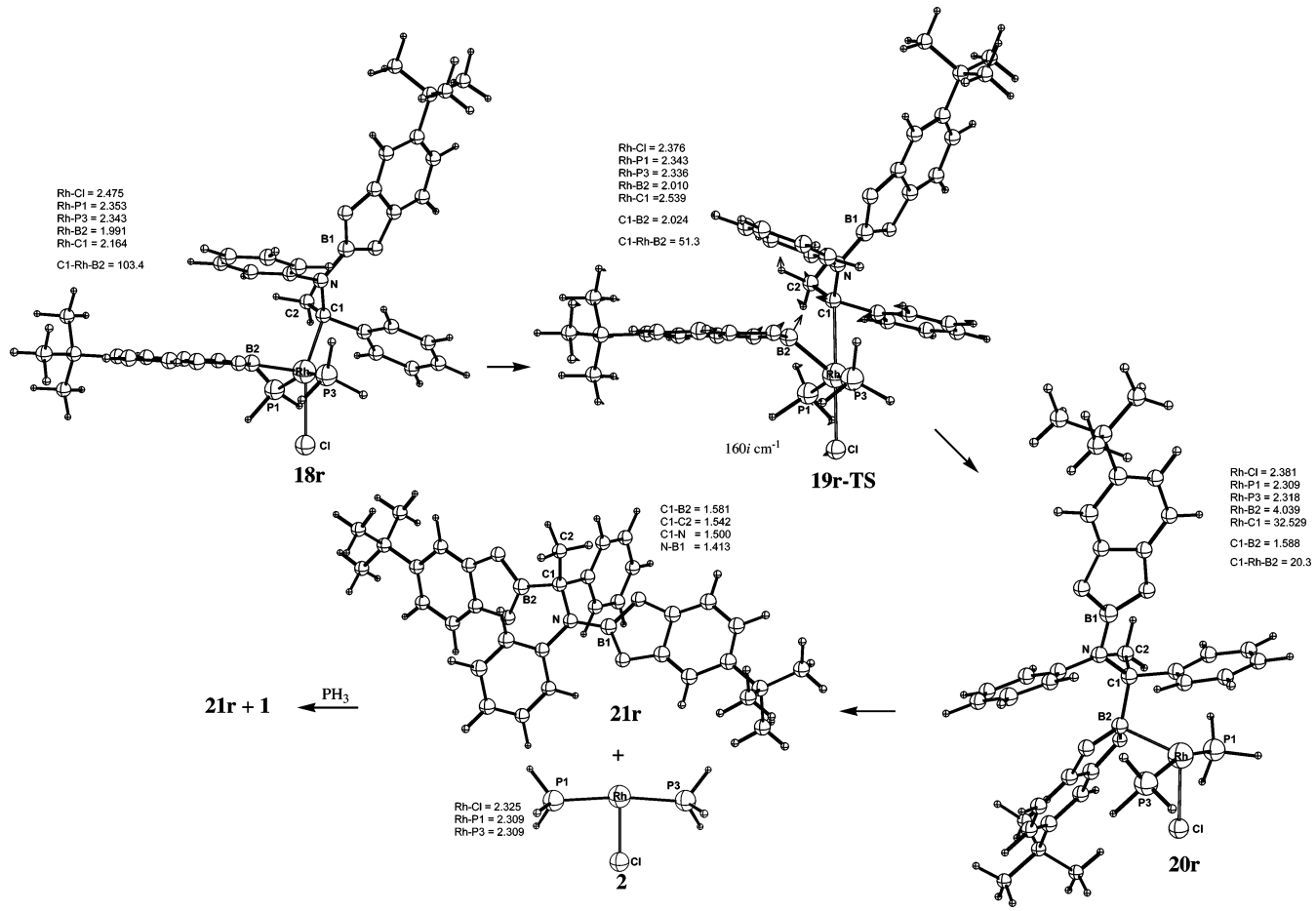

Figure 4. ONIOM-optimized geometry of stationary points **18r**−**21r** (distances in Å, angles in deg).

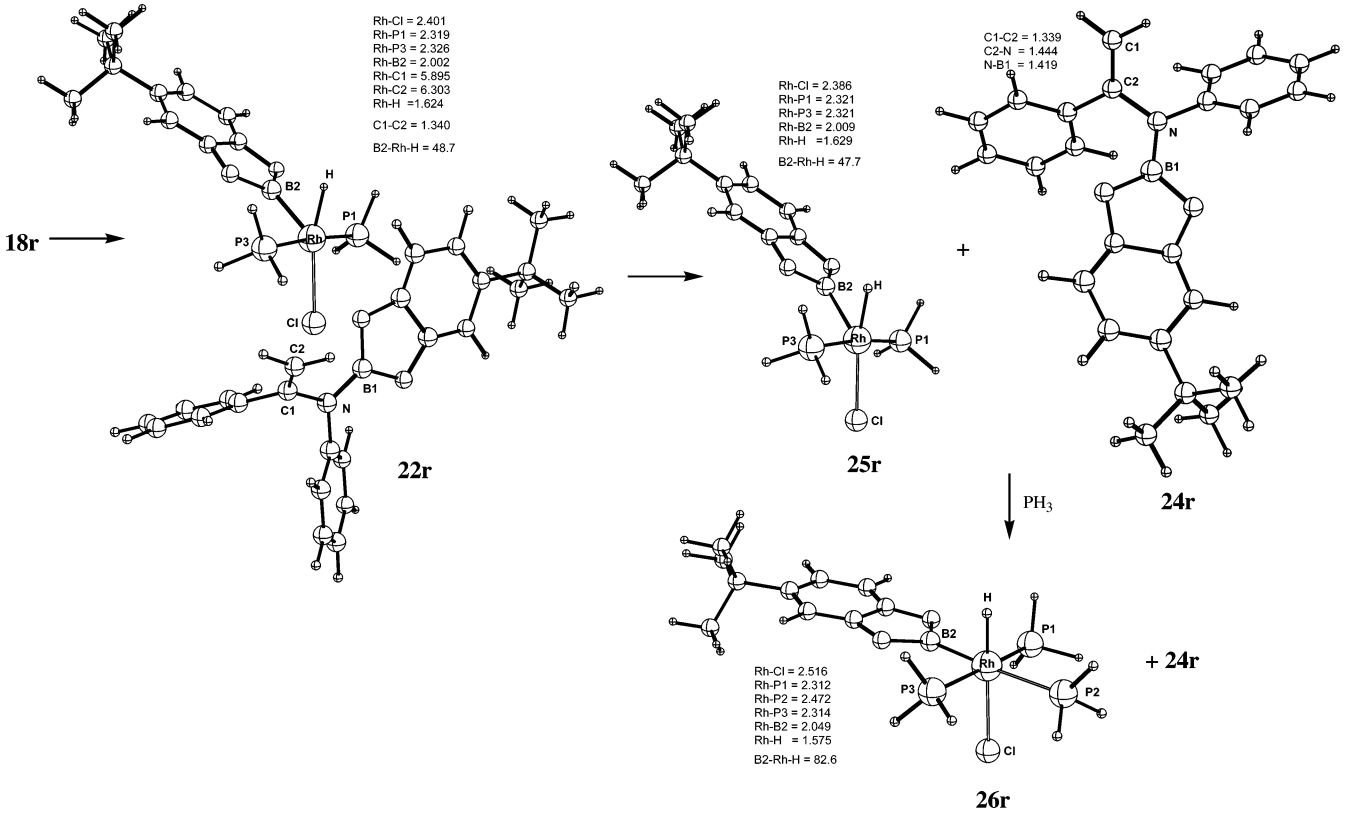

Figure 5. ONIOM-optimized geometry of stationary points **22r** and **24r**−**26r** (distances in Å, angles in deg).

Scheme 3. Mechanisms of Alkene (left) and Imine (right) Coordination and Insertion into the Metal−Boron Bond

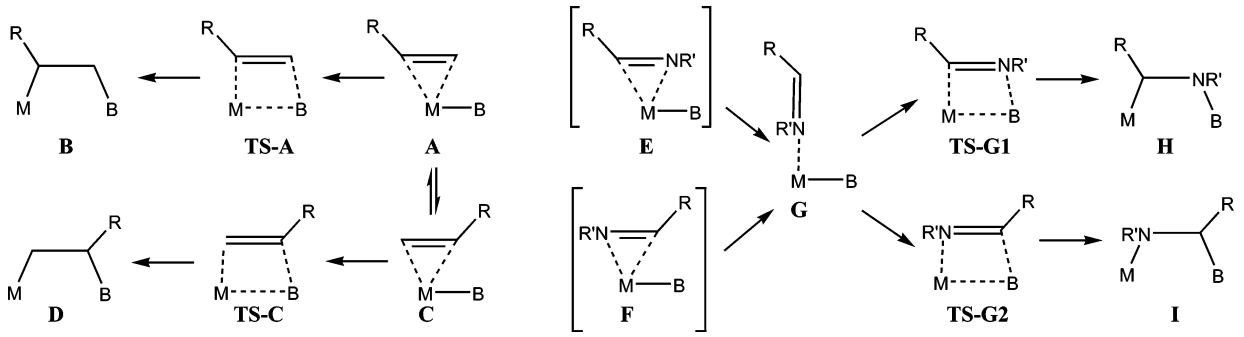

clearly give only the monoboration product for this reaction, which will be reexamined in the following section.

The experimentally reported C=N monoboration product **24** may be reached from either **15** or **18** via a β-hydride elimination (Figure 2). The barrier for this reaction is too low, and we were unable to locate the transition state for this C−H bond activation by rhodium. This is in agreement with earlier theoretical findings of very low barrier or even barrierless reaction for C−H bond activation.[20,21] The product of the β-hydride C−H bond activation, complex **22**, is only 1.1 (1.8) and 0.2 (0.6) kcal/mol higher in energy than the prereaction complexes **15** and **18**, respectively. It is not surprisingly that complex **23**, an isomer of complex **22,** is 26.3 (24.9) higher in energy than **22** (Table 1), due to having two ligands, B and H, with strong *trans* effect in *trans* positions to each other. Dissociation of the π-complex **22** to release the final product **24**, leaving behind the hydride complex **25**, is exothermic by 10.1 (−1.3) kcal/mol.

At the next stage, the five-coordinated compound **25** may coordinate the PH_3 ligand and form complex **26**. This step is unfavorable on the ΔG surface; however it is favorable on the ΔH surface (Table 1). Experimental studies have shown that the five-coordinated complex (analogue of **25**) rather than the six-coordinated complex (analogue of **26**) is formed after H−B addition to Rh(I).[22] Therefore, the calculated free energy surface provides

(20) (a) Koga, N.; Morokuma, K. *J. Phys. Chem.* **1990**, *94*, 5454. (b) Musaev, D. G.; Morokuma, K. *J. Am. Chem. Soc.* **1995**, *117*, 799.

(21) For general reviews see: (a) Didieu, A. *Chem. Rev.* **2000**, *100*, 543. (b) Musaev, D. G.; Morokuma, K. *Top. Catal.* **1999**, *7*, 107. (c) Siegbahn, P. E. M.; Blomberg, M. R. A. In *Theoretical Aspects of Homogeneous Catalysis*, *Applications of Ab Initio Molecular Orbital Theory*; van Leeuwen, P. W. N. M.. van Lenthe, J. H.. Morokuma, K.. Eds.; Kluwer Academic Publishers: Dordrecht, 1995. (d) Koga, N.; Morokuma, K. *Chem. Rev.* **1991**, *91*, 823.

(22) (a) Lam, W. H.; Shimada, S.; Batsanov, A. S.; Lin, Z.; Marder, T. B.; Cowan, J. A.; Howard, J. A. K.; Mason, S. A.; McIntyre, G. J. *Organometallics* **2003**, *22*, 4557. (b) Shimada, S.; Batsanov, A. S.; Howard, J. A. K.; Marder, T. B. *Angew. Chem., Int. Ed.* **2001**, *40*, 2168.

Scheme 4. Mechanism of Catalytic Imine Boration Reaction Derived from the Present Calculations (L = PH_3)[a]

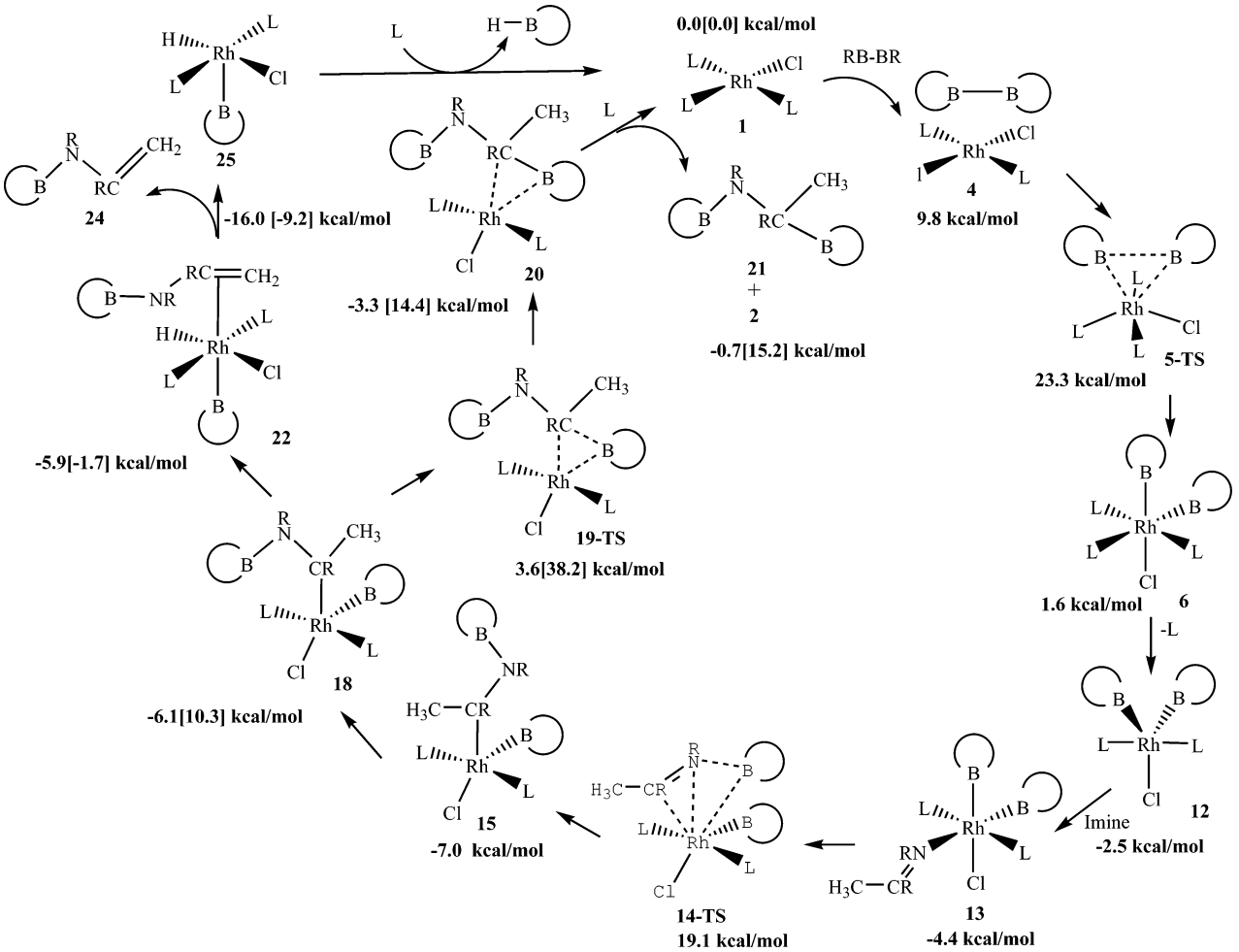

[a] The relative ΔG values for the model system, $(H_2C_2O_2)B-B(H_2C_2O_2)$ and $HN=C(H)CH_3$, as well as for the real system, Cat′B−BCat′ and $PhN=C(Ph)CH_3$ (in brackets), are shown.

the correct description of the relative stability of transition metal complexes and **25** + **24** should be considered as the final point of the monoboration reaction.[23] Compared to the initial point **1** the formation of monoboration (**24** + **25**) products is exothermic by 16.0 (19.3) kcal/mol (Table 1), providing the necessary driving force for the reactions.

The overall catalytic cycle derived from the present calculations is shown in Scheme 4. The graphical representation of the potential energy surface is given in Figure 3.

Comparison of the above presented results for the catalytic model reaction with the available experimental data[10] shows that they are in agreement only in part. In particular, (1) calculations and experiment show that the stoichiometric reaction of RB−BR and $[RhCl(PPh_3)_3]$ leads to the oxidative addition product $[RhCl(BR)_2(PPh_3)_2]$, complex **12**, which is the most stable oxidative addition product on the ΔG surface (Table 1); (2) calculations, like the experiments, have provided evidence for formation of the $[RhHCl(BR)(PPh_3)_2]$ hydride complex and monoboration products, and (3) the calculations correctly predict the regioselectivity (**G** → **H** and **G** → **I**) of the insertion step in the catalytic reaction.

However, the model study failed to explain the most important feature of the experimentally reported Rh-catalyzed imine C=N boration. According to the calculations, both diboration (**21**) and monoboration (**24**) products can be formed, while only selective formation of the monoboration species was observed in the experimental reactions.

To elucidate the reasons for these discrepancies between the calculated and experimental results, we will now include into the calculations the entire substrate molecules without any truncation and recalculate the processes starting from the complex **18**, namely, **18** → **19-TS** → **20** and **18** → **22** → **24** + **25** (Scheme 3) using the ONIOM method. One should mention that the process involving elementary steps **18** → **19-TS** → **20** leads to the diboration product, while that with **18** → **22** → **24** + **25** gives the monoboration product.

B. ONIOM Studies for the Real Substrates. The ONIOM-calculated energies of these reactions are presented in Table 1 and Figure 3, while the optimized structures of the possible intermediates, transition states, and products are given in Figures 4 and 5.

Now we are using the entire borane (Cat′B−BCat′) and the entire imine ($PhN=C(Ph)CH_3$) molecules in-

(23) Under experimental conditions the hydride complex **25** may also catalyze C=C bond hydroboration of the final product **24** (see ref 6). We will not repeat the theoretical investigation of the alkene hydroboration, since it has been reported previously (see ref 4).

stead of $(H_2C_2O_2)B-B(H_2C_2O_2)$ and $HN{=}C(H)CH_3$ as their models, while we still use PH_3 as phosphine. Table 1 shows that the activation barrier of the C−B reductive elimination reaction is increased drastically for the entire "real" substrates, compared with the results for the model substrates. For the process **18r** → **19r-TS** → **20r** (here and below "**r**" after the structure number stands for the "real" system, and brackets are used for energies of the "real" system) leading to the diboration product, the barrier at the transition state **19r-TS** is [27.9 (26.3)] kcal/mol compared to 9.7 (7.3) kcal/mol at the transition state **19-TS** of the model system.

The most likely reason for the increased barrier is repulsion between the bulky groups of the substrates. The steric strain is reflected by the C1−Rh−B2 angle in complex **18r**: 103.4° compared to 80.9° in the model system **18** (cf. Figures 2 and 4). Reflecting the same steric congestion, the overall C−B bond formation process **18r** → **19r-TS** → **20r** is found to be endothermic by [4.1 (8.2)] kcal/mol for the real substrates, while the model process **18** → **19-TS** → **20** is calculated to be only slightly endothermic by 2.8 (1.5) kcal/mol.

It is important to notice, however, that the bulkiness of organic substituents does not introduce additional energy demand to the β-hydrogen elimination, i.e., the **18r** → **22r** → **24r** + **25r** process that leads to monoboration products. Geometry optimization of the C−H bond activation product in the real system resulted in weak van der Waals complex **22r**, instead of the π-complex found in the model study (cf. Figures 2 and 5). In agreement with the model system, we were not able to locate the transition state of the C−H bond activation. Complex **22r** is more stable than **18r** by [12.0 (6.1)] kcal/mol, while **22** is less stable than **18** by 0.2 (0.6) kcal/mol. Both diboration (**21r** + **1**) and monoboration (**24r** + **25r**) reactions are exothermic by [13.5 (28.9)] kcal/mol and [9.2 (13.5)] kcal/mol, respectively, relative to the reactants **1** + $PhN{=}C(CH_3)Ph$ + Cat′B−BCat′.

Thus, according to the ONIOM calculations, the inclusion of the electronic and steric effects of the substrate substituents significantly destabilizes the diboration process and favors the monoboration process. As a result, the β-hydrogen elimination pathway leading to the monoboration product becomes the only feasible pathway for the reaction of Rh(I)-catalyzed $PhN{=}C(CH_3)Ph$ C=N bond boration using Cat′B−BCat′. The result with the real substrates is in excellent agreement with the experimental study.[10] *Thus, these calculations predict that bulkiness of the imine and boration reagents is responsible for switching the direction of the catalytic reaction from diboration to monoboration.*

It is interesting to note that platinum-catalyzed addition of CatB−BCat to imines resulted in selective formation of the expected diboration product.[24] This fact is in qualitative agreement with the present study, since much higher activation barriers were calculated for C−H activation by Pt complexes,[21,25] while C−B reductive elimination from Pt complexes can proceed easily.[8] Therefore, it is a unique feature of Rh complexes that allows unusual monoboration of imines.

4. Conclusions

From the present study the following main conclusions can be drawn:

(i) Due to easy C−H activation by Rh complexes, two competitive routes are possible in the imines boration reaction: C−B reductive elimination leading to a diboration product and β-hydrogen elimination resulting in a monoboration product.

(ii) It is the sterical effect of the substrates that controls the direction of the catalytic reaction; bulky ligands retard the C−B reductive elimination, while β-hydrogen elimination is not influenced significantly.

(iii) The catalytic reaction of $PhN{=}CPhCH_3$ imine boration with Cat′B−BCat′ includes the following stages: (1) oxidative addition of B−B to the Rh complex; (2) imine coordination; (3) migratory insertion of the imine into the Rh−B bond; and (4) β-hydrogen elimination.

(iv) Although the model calculations on the small model system may be utilized to construct the basic potential energy surface, the full-size system with the substituted substrates is required to take care of the steric effects and to obtain the potential energy profile consistent with the experiment. The steric effects of bulky substituents work as an internal switch for the mechanistic change.

(v) The difference between alkene and imine boration has been identified. For alkenes two coordination orientations lead to different regio products, while for imines the single possible coordination mode exclusively gives Rh−C and N−B bond formation. Thus higher regioselectivity should be expected for imine boration.

To the best of our knowledge the present study is the first to report a theoretical calculation that correctly predicts the direction of the catalytic boration reaction depending on the nature of the substrates.

Acknowledgment. V.P.A. acknowledges the Visiting Fellowship from the Emerson Center and is grateful for the access to computational resources provided by the Cherry L. Emerson Center of Emory University. The present research is in part supported by a grant (CHE-0209660) from the National Science Foundation.

Supporting Information Available: Figure S1: Optimized geometry of imine and boration reagent (in Å and deg). Figure S2: Optimized geometry of stationary points **27**−**30** (in Å and deg); for each stationary point ΔG (ΔH in parentheses, in kcal/mol) values are given. Figure S3: Optimized geometry of stationary points **31**−**32** (in Å and deg); for each stationary point ΔG (ΔH in parentheses, in kcal/mol) values are given, and complete ref 17.

OM049156O

(24) Mann, G.; John, K. D.; Baker, R. T. *Org. Lett.* **2000**, *2*, 2105.

(25) (a) Sakaki, S.; Mizoe, N; Musashi, Y.; Biswas, B.; Suginoto, M. *J. Phys. Chem.* **1998**, *102*, 8027. (b) Obara, S.; Kitaura, K.; Morokuma, K. *J. Am. Chem. Soc.* **1984**, *106*, 7482.